http://dx.doi.org/10.21577/0103-5053.20180213

J. Braz. Chem. Soc., Vol. 30, No. 4, 813-818, 2019
Printed in Brazil - ©2019 Sociedade Brasileira de Química

Article

Photochemical Synthesis of Gold Nanoparticles by Irradiation of Gold Chloride with the 2nd Harmonic of a Nd:YAG Laser

Henrique F. P. Barbosa,[a] Miguel G. Neumann[a] and Carla C. S. Cavalheiro[*,a]

[a]*Instituto de Química de São Carlos, Universidade de São Paulo, CP 780, 13560-970 São Carlos-SP, Brazil*

A synthesis method was developed capable of obtaining pristine gold nanoparticles (AuNPs) using the lowest possible amount of auxiliary compounds. An aqueous solution of $HAuCl_4.3H_2O$ was irradiated, in the absence of any stabilizing species, with the 532-nm radiation of a Nd:YAG laser. Spherical shaped AuNPs were produced by this method with sizes below 10 nm. The crystalline structures were stable for up to 28 days. A mechanism for this process is also proposed based on the initial cleavage of water molecules by the laser irradiation followed by the formation of hydrogen peroxide that reduces the gold species Au^{III}. The resulting species of these reactions (H_2 and O_2) were identified by mass spectrometry. This new method suggests that laser irradiation is a feasible alternative to produce ready-to-use AuNPs, for drug delivery, diagnostics or bio-imaging.

Keywords: gold nanoparticles, nanoparticle photochemical synthesis, Nd:YAg laser

Introduction

Nanomaterials have attracted the interest of many researchers in the last few years due to their properties and applications. For instance, gold nanoparticles can be used as drug delivery system, delivering drugs with more efficiency and diminishing their side effects.[1] In spintronics, doped nanoparticles are used to increase the efficiency of LEDs and lasers.[2] Magnetic nanoparticles can enhance the detection of cancer through magnetic resonance imaging.[3]

Two approaches are generally used to synthesize nanomaterials: top-down and bottom-up paths. The top-down path methods start with a macro sized material which is broken down in smaller pieces until their dimensions are in the nanometer scale. On the other hand, the bottom-up methods start with single atoms that are agglomerate until particles in the nanometer scale are formed.[4] Comparing both methods, it can be concluded that synthesis via bottom-up presents some advantages, such as more homogenous chemical composition and surfaces with less defects.[4]

Gold nanoparticles have been studied due to their vast application range, such as in packaging,[5] catalysis,[6] sensing,[7] solar energy harvesting,[8] drug delivery,[9] data storage,[10] diseases diagnostics[9] and electric conductivity.[11]

*e-mail: carla@iqsc.usp.br

Its properties applications are due to some specific characteristics as size, surface area, morphology and composition, which are influenced by the synthesis method. Although many methods are used to obtain these nanoparticles, the vast majority rely in the use of auxiliary compounds, such as reducing agents, catalyzers and stabilizers, which may hamper or make them useless for further applications.[12-15]

Bottom-up syntheses, which involve the lowest possible number of auxiliary compounds allowing the obtainment of pristine Au nanoparticles (AuNPs) with good control of size and morphology are desirable. Several methods have been used towards this goal. By instance, reduction of gold(III) solutions using UV-irradiation[16] or irradiation of similar gold solutions by pulsed lasers.[17,18] In general, these procedures rely on the presence of stabilizers, or even preselected capping species. The laser drop method devised by Scaiano and co-workers[19] involves the laser irradiation of a solution drop containing pre-formed gold particles originated by the mild reduction of a gold chloride solution by hydrogen peroxide. Also, pulsed laser irradiation on gold powder has been used to produce AuNPs.[20]

In this work we are presenting results for the synthesis of gold nanoparticles by the direct irradiation of a gold(III) chloride solution with the 532 nm wavelength emission of a Nd:YAG laser. This method allows the adjustment of a large number of parameters, so that an accurate control of

the AuNPs characteristics can be obtained. A mechanism for this procedure is also proposed.

The properties of the produced AuNPs were determined by UV-Vis spectrophotometry (UV-Vis), dynamic light scattering (DLS), transmission electron microscopy (TEM), selected area electron diffraction (SAED) and zeta potential (ZP).

Experimental

Materials and chemicals

Gold(III) chloride trihydrate ($HAuCl_4.3H_2O$-49%) was purchased from Sigma-Aldrich. Ultrapure water was obtained by purification system Barnstead EasyPureRoDi from Thermo Fisher Scientific. 1-cm quartz cuvettes utilized were from Hellma. The Nd:YAG laser system was a model Brilliant B from Quantel Laser used at the second harmonic wavelength, 532 nm. Pulse duration was 5.2 ns, at a repetition rate of 10 Hz, maximum pulse energy of 150 mJ, beam diameter of 0.9 cm.

Sample preparation

Aqueous stock solutions of $HAuCl_4.3H_2O$ (4×10^{-3} mol L^{-1}) were prepared using ultrapure water. Different amounts of these stock solutions were employed to prepare samples of 1 mL total volume with specific final concentrations (Table 1). All samples were prepared inside the quartz cuvettes.

Table 1. Concentration of the prepared samples

Sample	[$HAuCl_4$] / (mol L^{-1})
CT1	2.54×10^{-5}
CT2	2.54×10^{-4}
CT3	2.54×10^{-3}

Synthesis of nanoparticles

A 532 nm laser beam was directed onto the samples contained in a quartz cuvette under magnetic stirring for 4 h (including pulses and their intervals).

Characterization

To confirm the formation of nanoparticles, UV-Vis spectrophotometry (Shimadzu UV-2550) was carried out on the irradiated cells. Dynamic light scattering (Malvern Zetasizer Nano-ZS) was used to analyze the size and stability of the particles. Transmission electron microscopy and selected area electron diffraction (FEI TECNAI G2-F20) were performed to attest the morphology, size and crystalline structure of the nanoparticles. Mass spectrometry (Pfeiffer Vacuum Omnistar GSD 320) was used to confirm the liberation of specific gases during synthesis, in order to confirm the mechanism of the synthesis.

Results and Discussion

UV-Vis spectra

Samples CT1, CT2 and CT3 were prepared to determine the influence of the concentration of $HAuCl_4$ on the formation of the nanoparticles. The UV-Vis spectra of the irradiated samples are shown in Figure 1.

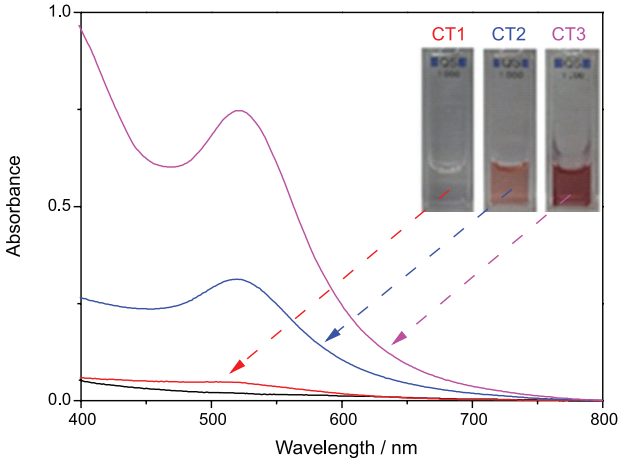

Figure 1. UV-Vis spectra of samples CT1 (2.54×10^{-5} mol L^{-1}), CT2 (2.54×10^{-4} mol L^{-1}) and CT3 (2.54×10^{-3} mol L^{-1}) after 4 h of 532 nm Nd:YAG laser irradiation.

It can be noticed that after 4 h irradiation, peaks appeared around 520 nm, confirming the production of AuNPs.[20-22] It can be seen that the higher concentration solutions resulted in larger peaks. This could indicate the production of more AuNPs or the production of AuNPs with larger sizes.[23]

TEM analysis

Figure 2 shows the TEM images of the 3 samples along with the corresponding size distribution.

It can be inferred from the TEM images that both CT1 and CT2 present AuNPs with spherical morphology whereas CT3 gives rise to particles with larger size and different morphologies, as can also be deduced from the UV-Vis spectra. The presence of different morphologies at higher concentrations was already reported in the literature.[23] The AuNPs obtained from the CT1 sample

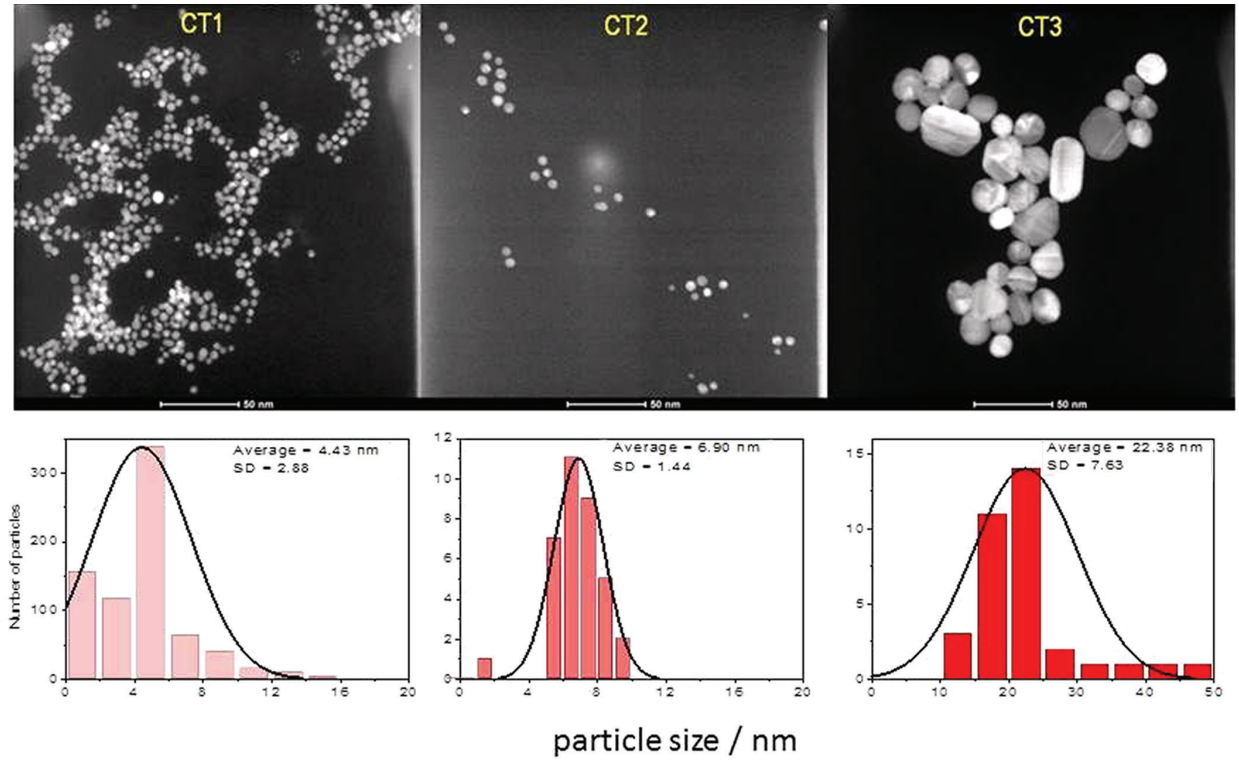

Figure 2. Transmission electron microscopy and size distributions of CT1, CT2 and CT3 AuNPs nanoparticles.

present smaller sizes and it seems likely that some of them suffered fusion. The fusion may be due to the plasma produced by the laser irradiation.[24]

The size of the nanoparticles was evaluated using the ImageJ software. When using the solution with lower $HAuCl_4$ concentration (CT1) the average size of the nanoparticles was 4.33 nm, whereas for the highest concentration (CT3) the size increased to 22.38 nm. Thus, it can be concluded that higher initial concentrations of $HAuCl_4$ will render larger AuNPs, when using the same irradiation conditions.

The AuNPs average sizes obtained are comparable to the sizes reported in previous studies.[12,21,18,25] This is remarkable considering that the particles obtained by this method do not involve stabilizers or surfactants.

SAED analysis

SAED characterization of all samples was performed and the obtained images are shown in Figure 3.

The crystalline planes corresponding to each ring were determined using the ImageJ software. All the samples presented crystal planes referring to the FCC crystalline structure, which is the most energetically stable for AuNPs.[26,27]

Stability

The stability of the nanoparticles was evaluated by the changes of the size (obtained by DLS) and the variations of the ZP during 4 weeks with the sample stored at low

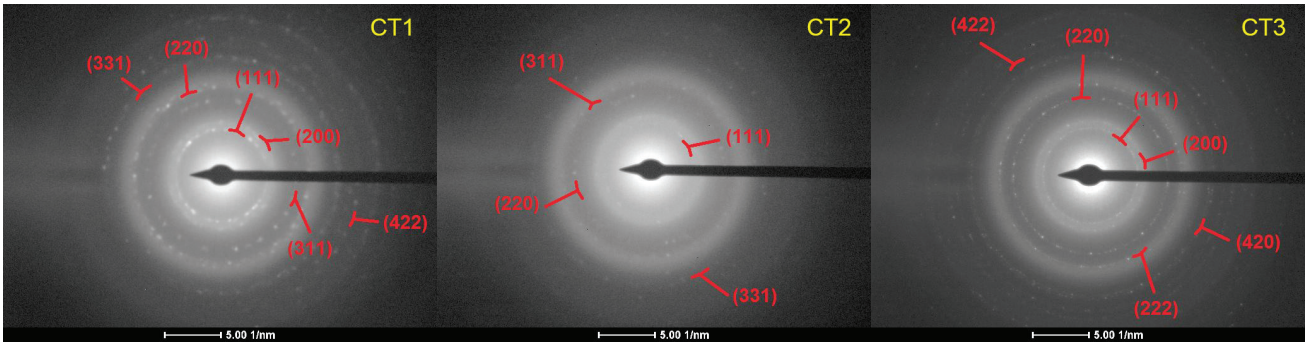

Figure 3. SAED images of the irradiated samples showing the crystalline planes.

temperature (4 ºC). The corresponding results, for the irradiated CT2 sample, are shown in Figure 4.

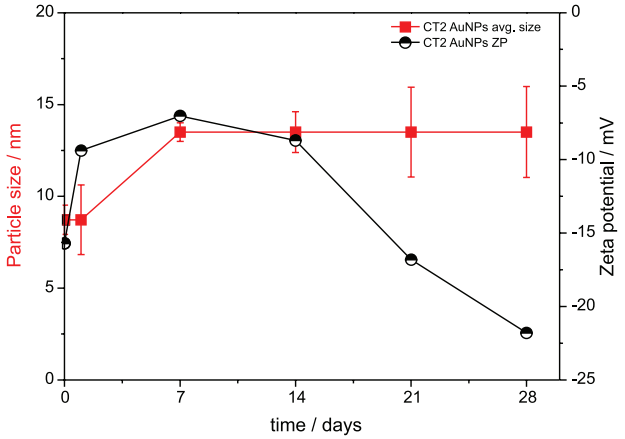

Figure 4. Average size and zeta potential variations of the CT2 AuNP over 28 days.

The sample was stored at low temperature (4 ºC) between measurements. It can be noticed that the average size of the AuNPs is maintained constant during the first 24 h. There is a marked increase between 24 h and 1 week when the size changed from ca. 7 to 12 nm. This size was maintained for, at least, the next four weeks. The size variation occurred along with a concomitant variation of the ZP. The initial increase of the ZP is coherent with the increase of the nanoparticles size. But, as its value moves away from the 0 mV value, the AuNP becomes more stable.[28]

In previous report,[29] it has been claimed that in the presence of stabilizers, the size of the AuNPs was kept around 20 nm for 20 days. Since no stabilizer was used in this work, the determined average size of 12 nm kept stable between the first and four weeks seems quite remarkable.

Mechanism

Synthesis of AuNPs was performed through irradiation of the samples with a Nd:YAG laser using the 2nd harmonic wavelength (532 nm). The acting mechanism is due to reactions originated from the interactions of the laser beam with water and the gold compound $HAuCl_4$.

The working conditions in this research are similar to those used by Chin and Lagacé[24] using a Ti-sapphire laser. The plasma originated by the interaction of the laser beam with water leads to the scission of an O–H bond, generating free radicals that will recombine to form H_2, O_2 and H_2O_2.

$$H_2O \xrightarrow{\text{laser}} H^{\bullet} + OH^{\bullet} \quad (1)$$

$$H^{\bullet} + OH^{\bullet} \rightarrow \left[H_2;\ O_2;\ H_2O_2\right] \quad (2)$$

The formed H_2O_2 can further dissociate into H_2O and $O^{\bullet}$ in the plasma, the latter giving rise to molecular oxygen.

$$H_2O_2 \xrightarrow{\text{laser}} H_2O + O^{\bullet} \quad (3)$$

In their study of the synthesis of gold nanoparticles Tibbetts *et al.*[18] proposed similar reactions, but considered that the laser beam could generate hydrated electrons. Nevertheless, the final products would remain the same.

$$H_2O \xrightarrow{\text{laser}} e^-_{aq} + H^+ + OH^{\bullet} \quad (4)$$

In order to prove the presence of the products resulting from the water splitting process, mass spectra of the CT2 sample were performed before and after irradiation (Figure 5).

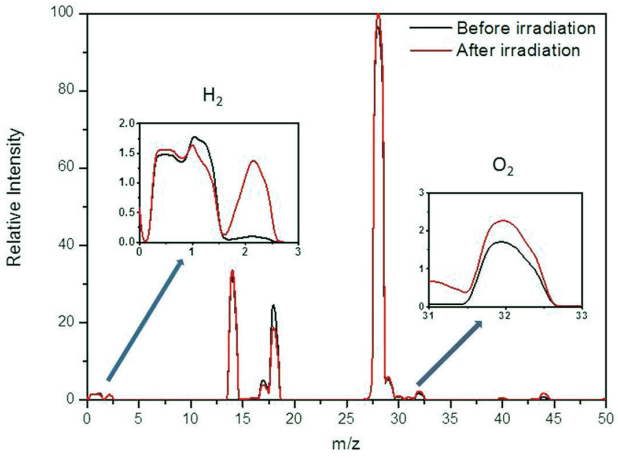

Figure 5. Mass spectra of CT2 before and after 532 nm irradiation of a Nd:YAG laser. Insets show the amplification of the signals corresponding to H_2 and O_2.

As can be seen in the insets of Figure 5, there is an increase of H_2 (at *m/z* 2) and O_2 (at *m/z* 32) after irradiation, confirming the formation of these two water splitting species after irradiation:

$$6H_2O \xrightarrow{\text{laser}} 8H^{\bullet} + 2O^{\bullet} + 4OH^{\bullet} \quad (5)$$

$$8H^{\bullet} + 2O^{\bullet} + 4OH^{\bullet} \longrightarrow 4H_2 + O_2 + 2H_2O_2 \quad (6)$$

Regarding the interaction between the laser radiation and $HAuCl_4$, Tibbets *et al.*[18] proposed a mechanism that involved the photolytic direct split of water, formation of hydrated electrons and autocatalysis due to the formed hydrogen peroxide. The overall reactions corresponding to these processes can be seen below:

$$H_2O \xrightarrow{\text{laser}} e^-_{aq} + H^+ + OH^{\bullet} \quad (7)$$

$$H_2O \xrightarrow{laser} H^{\bullet} + OH^{\bullet} \quad (8)$$

$$\left[Au^{III}Cl_4\right]^- + 3e^-_{aq} \rightarrow Au^0 + 4Cl^- \quad (9)$$

$$\left[Au^{III}Cl_4\right]^- + 3H^{\bullet} \rightarrow Au^0 + Cl^- + 3HCl \quad (10)$$

On the other hand, Shang *et al*.,[16] during their study of the reduction of $HAuCl_4$ by UV irradiation, proposed a direct photochemical reduction of the Au^{III} complex to the Au^{II} complex, which, in turn, would disproportionate into Au^{III} and Au^{I}, and a final photochemical reduction of the latter. As in that work, the irradiation method involved only a conventional high pressure UV lamp, no hydrated electrons would be present. But, when adapting this mechanism to that processed through highly energetic intense laser radiation, the acting mechanism could be assumed to be:

$$\left[HAu^{III}Cl_4\right] \rightarrow H^+ + \left[Au^{III}Cl_4\right]^- \quad (11)$$

$$\left[Au^{III}Cl_4\right]^- + e^-_{aq} \rightarrow \left[Au^{II}Cl_3\right]^- + Cl^{\bullet} \quad (12)$$

$$2\left[Au^{II}Cl_3\right]^- \rightarrow \left[Au^{III}Cl_4\right]^- + \left[Au^{I}Cl_2\right]^- \quad (13)$$

$$\left[Au^{I}Cl_2\right]^- \rightarrow Au^0 + Cl^{\bullet} + Cl^- \quad (14)$$

Although the mechanisms above indicate the formation of Cl_2 after irradiation, it was not observed in the mass spectra experiments (through the concomitant presence of $Cl^{\bullet}$ at 35 μ), possible due to the rather low concentration of $HAuCl_4$ (ca. 10^{-4} mol L^{-1}). Therefore, considering that Cl_2 is being really produced and knowing that the proposed laser-water interaction mechanism produces all the compounds indicated through reactions 7, 8 and 9 to occur, it can be concluded that the indicated mechanism leading to gold nanoparticles also occurs when irradiating $HAuCl_4$ with the second harmonic of the Nd:YAG laser at 532 nm.

Conclusions

A new bottom-up synthesis method for gold nanoparticles was proposed in this paper showing promising results. The obtained AuNPs presented average sizes around 10 nm, stable crystalline structure and spherical morphology, characteristics comparable to those found at nanoparticles obtained by other methods. A considerable stability was also obtained for the synthesized AuNPs, even in the absence of surfactants and stabilizers. This indicates their potential to produce ready-to-use nanoparticles.

Acknowledgments

This research was financially supported by Conselho Nacional de Desenvolvimento Científico e Tecnológico (CNPq), grants No. 401434/2014-1 and 490421/2013-0. C. C. S. C. and M. G. N. thank CNPq for respective research fellowships. H. F. P. B. thanks Coordenação de Aperfeiçoamento de Pessoal de Nível Superior (CAPES) for a graduate studentship.

References

1. Dreaden, E. C.; Austin, L. A.; Mackey, M. A.; El-Sayed, M. A.; *Ther. Delivery* **2012**, *3*, 457.
2. Chen, W.; Zhang, J. Z.; Joly, A. G.; *J. Nanosci. Nanotechnol.* **2004**, *4*, 919.
3. Sun, C.; Lee, J. S. H.; Zhang, M.; *Adv. Drug Delivery Rev.* **2008**, *60*, 1252.
4. Cao, G.; Wang Y.; *Nanostructures and Nanomaterials Synthesis, Properties, and Applications*; World Scientific: New Jersey, USA, 2011.
5. Honarvar, Z.; Hadian, Z.; Mashayekh, M.; *Electron. Physician* **2016**, *8*, 2531.
6. Daniel, M. C.; Astruc, D.; *Chem. Rev.* **2004**, *104*, 293.
7. Priyadarshini, E.; Pradhan, N.; *Sens. Actuators, B* **2017**, *238*, 888.
8. Torres-Mendieta, R.; Mondragón, R.; Puerto-Belda, V.; Mendoza-Yero, O.; Lancis, J.; Juliá, J. E.; Mínguez-Vega, G.; *ChemPhysChem* **2017**, *18*, 1055.
9. Kong, F.-Y.; Zhang, J. W.; Li, R. F.; Wang, Z. X.; Wang, W. J.; Wang, W.; *Molecules* **2017**, *22*, 1445.
10. Reiss, G.; Hütten, A.; *Nat. Mater.* **2005**, *4*, 725.
11. Ma, C.; Tang, B. Z.; Kim, J.-K.; *Carbon* **2008**, *46*, 1497.
12. Turkevich, J.; Stevenson, C.; Hillier, J.; *Discuss. Faraday Soc.* **1951**, *11*, 55.
13. Brust, M.; Walker, M.; Bethell, D.; Schiffrin, D. J.; Whyman, R.; *J. Chem. Soc., Chem. Commun.* **1994**, 801.
14. Dong, S.; Tang, C.; Zhou, H.; Zhao, H.; *Gold Bull.* **2004**, *37*, 187.
15. Pileni, M.; *Nat. Mater.* **2003**, *2*, 145.
16. Shang, Y.; Min, C.; Hu, J.; Liu, H.; Hu, Y.; *Solid State Sci.* **2013**, *15*, 17.
17. Meader, V. H.; John, M. G.; Rodrigues, C. J.; Tibbetts, K. M.; *J. Phys. Chem. A* **2017**, *121*, 6742.
18. Tibbetts, K. M.; Tangeysh, B.; Odhner, J. H.; Levis, R. J.; *J. Phys. Chem. A* **2016**, *120*, 3562.
19. Bueno-Alejo, C. J.; D'Alfonso, C.; Pacioni, N. L.; González-Béjar, M.; Grenier, M.; Lanzalunga, O.; Alarcon, E. I.; Scaiano, J. C.; *Langmuir* **2012**, *28*, 8183.
20. Lee, J.; Lee, M.; *J. Phys. Chem. C* **2016**, *120*, 13256.
21. Binaymotlagh, R.; Hadadzadeh, H.; Farrokhpour, H.; Haghighi,

F. H.; Abyar, F.; Mirahmadi-Zare, S. Z.; *Mater. Chem. Phys.* **2016**, *177*, 360.
22. Song, J.; Hwang, S.; Park, S.; Kim, T.; Im, K.; Hur, J.; Nam, J.; Kim, S.; Park, N.; *RSC Adv.* **2016**, *6*, 51658.
23. Anyfantis, G. C.; Scotto, M.; Scarpellini, A.; Pignatelli, F.; Toussi, S. M.; Ruffilli, R.; Martiradonna, L.; Athanassiou, A.; *Part. Part. Syst. Charact.* **2015**, *32*, 389.
24. Chin, S. L.; Lagacé, S.; *Appl. Opt.* **1996**, *35*, 907.
25. Tetsu, Y.; Mizuki, S.; Toyoki, K.; *Chem. Lett.* **1997**, *26*, 619.
26. Shim, J.-H.; Lee, S.-C.; Lee, B.-J.; Suh, J.-Y.; Choet, Y. W.; *J. Cryst. Growth* **2003**, *250*, 558.
27. Callister, W. D.; Rethwisch, D. G.; *Materials Science and Engineering*, *SI Version*, 8th ed.; John Wiley & Sons, Inc: New York, 2011.
28. Bhattacharjee, S.; *J. Controlled Release* **2016**, *235*, 337.
29. Balasubramanian, S. K.; Yang, L.; Yung, L. Y.; Ong, C. N.; Ong, W. Y.; Yu, L. E.; *Biomaterials* **2010**, *31*, 9023.

Submitted: August 21, 2018
Published online: October 26, 2018